Supplementary Information

Experimental setup:

Laser

We used an integrated "Analyte fs" system (Photon Machines, San Diego, CA, USA), which includes a diode-pumped Ti:Sapphire femtosecond source, a Chirped Pulse Amplification system, and a third harmonic generator (THG) that converts the fundamental emission (λ=800nm) into near-UV (λ=266nm). Table S1 in the supporting information shows the complete settings. The system produces τ~150fs pulses at 900μJ/pulse with an adjustable repetition rate from 1 to 250Hz. The spot size is controlled by a set of masks, and the beam is delivered to the sample through an imaging aperture, giving 30μJ/pulse, taking into account transmission losses. The fluence on the sample is ~ 1J.cm^{-2} for a spot size of 12μm. The ablation cell is a new generation two-volume model (Photon Machines/Cetac "HelEx") [24] that provides a wash out of ~0.7s under a ~0.6Lmin^{-1} flux of Helium. Raster mode was used at a speed of 2μm.s^{-1} and a repetition rate of 25Hz. This set up produces an Fe removal rate (See Table S2) that is equivalent to this calculated for LA-MC-ICP-MS analyses (5-10Hz and 1μm.s^{-1})[12]. The high repetition rate does not induce any catastrophic ablation and produces ~5μm deep trenches, as shown by SEM and white light interferometry (Figure S1).

Laser ablation				
	System	Photon Machine "Analyte-fs"		
	Source laser	Diode pumped Ti-Sapphire Quantronix "Darwin"		
	Warm up	~45 min		
	Pulse duration	~150 fs		
	Max energy	~900 μJ at Third Harmonic Generator output		
	Carrier gas	Helium		
	Ablation cell	Two volume		
	Wavelength	266 nm		
	Ablation mode	Rastering		
	Repetition rate	25 Hz		
	Spot size	12 μm		
	Fluence on sample	~1 $J.cm^{-2}$		
	Fe removal rate	~2.10^{-5} $\mu g.shot^{-1}.J^{-1}.cm^2$		
Aerosols collection		**for Isotope analysis**	**for SEM**	**for TEM**
	Substrate	Whatman (PTFE)	Millipore "Isopore™" (Polycarbonate)	TEM holder
	Helium flow	0.5 $L.min^{-1}$	0.5 $L.min^{-1}$	0.6 $L.min^{-1}$
	Argon mixing	29 $L.min^{-1}$	29 $L.min^{-1}$	~2.5 $L.min^{-1}$

Table S1: Summary of the laser parameters and aerosols collections settings. The Third Harmonic Generator (THG) produces a wavelength of 266nm from the fundamental 800nm generated by the Ti:Sapphire crystal. The fluence is calculated from the energy transmitted through the beam train, which is usually 10 to 20% of the maximum energy at THG.

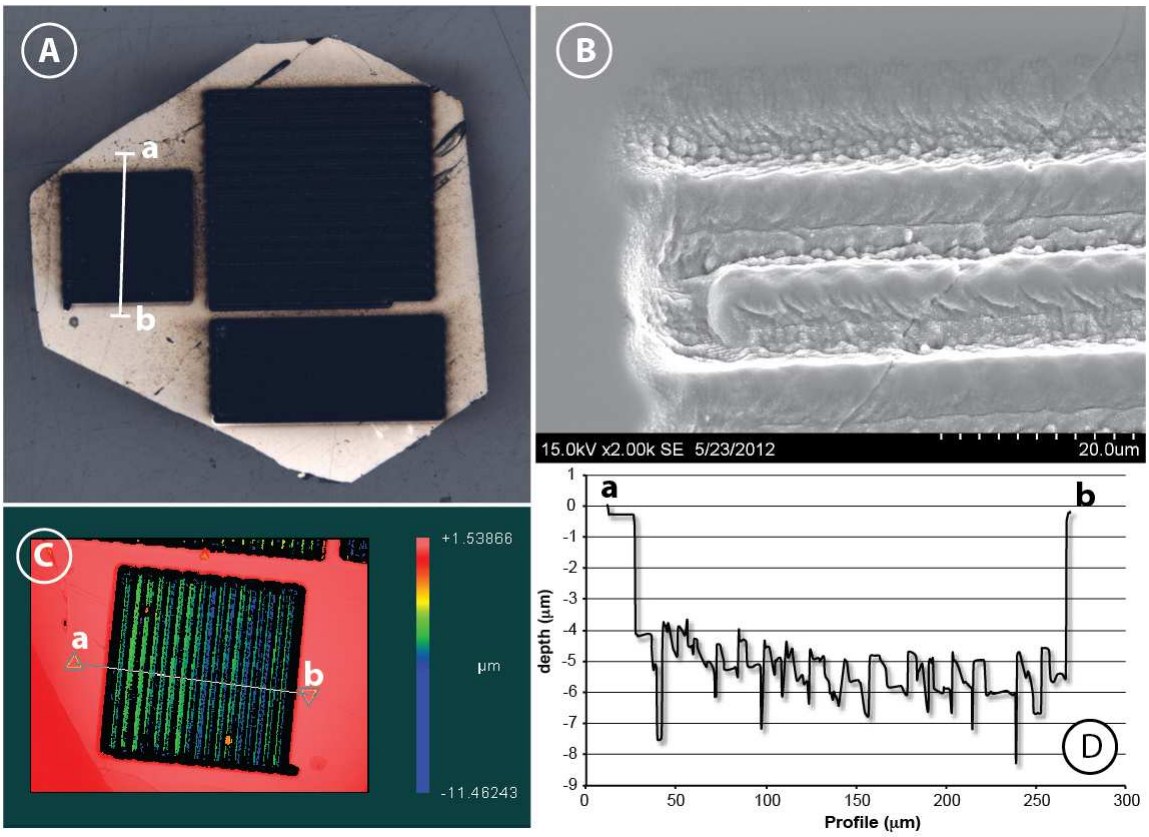

Figure S1: Optical microscope (A) and SE-SEM (B) images as well as white light interferogram (C) of femtosecond laser ablation of magnetite using raster mode at 25Hz and 2μm.s^{-1} at a fluence of ~1$J.cm^2$. No evidence for catastrophic ablation or melting could be found over all the ablated grains. White light interferometry allows an estimation of the ablation depth of ~5μm along the profile a-b plotted in (D).

Aerosol collection

A Micro-orifice Uniform Deposit Impactor (MOUDI) [25] was connected inline to the output from the ablation cell. The apparatus operates under a constant 30Lmin^{-1} flow rate. The Helium flow from the ablation cell was joined by a ~29.4Lmin^{-1} Argon flow using a "T" connector. Aerosol size sorting is achieved by the mean of pressure differences between the successive stages, which in turn affects the velocities of particles and their impact on each stage relative to particle kinetic energy. Consequently, the largest aerodynamic diameters are impacted on the first stages and the finest on the last. For isotope analysis, aerosols were collected on PTFE membranes (Whatman, 2μm porosity) placed on the twelve juxtaposed removable stages: the inlet, ten consecutive plates, and the filter stage. For particles analyzed by Scanning Electron Microscopy, collection used polycarbonate membranes (Millipore "Isopore^{tm}", 0.2μm porosity) that are resistant to the electron beam and have suitable elemental composition for SEM analysis. All particle sizes are reported as aerodynamic diameters (d_a), a quantity that is independent of particle density and shape factors. Conversion of d_a to a geometric diameter is not possible because particle morphologies can be very complex, and density is variable and dependent upon particle composition [46]. For particles analyzed by Transmission Electron Microscopy, collection was done over ~3h using copper sample holders d'Abzac *et al.* [31], and required mixing with only ~2.5L.min^{-1} Ar flow after the cell to avoid over pressurizing the apparatus. Details for each collection are reported in Tables S1 and S2 in the Supporting information.

		Experiment	120625	120627	120726	121026	121026	130408	130206	130206	130206
		Mineral	Py	Py	Mt	Py	Sid	Po	Mt	Py	Sid
		Duration (h)	21.5	25	25	27	34	34	2	2.7	3
		Fe removal rate (x10^{-5})	1.8	2.5	1.5	1.5	0.8	1.5	-	-	-
		Purpose	IA	IA	IA	IA	IA	IA	TEM	TEM	TEM
		Substrate	PTFE	PTFE	PTFE	PTFE	PTFE	PTFE	Cu grid	Cu grid	Cu grid
Impactor stage	Size class (μm)										
After filter	<0.056	Fe mass (μg)	6.46	13.50	7.24	2.43	3.87	4.15	-	-	-
10	0.056-0.1		2.42	5.29	2.27	2.22	1.36	1.59	-	-	-
9	0.1-0.18		16.47	18.69	10.08	14.76	6.69	16.41	-	-	-
8	0.18-0.32		3.07	6.17	5.07	7.28	2.82	11.15	-	-	-
7	0.32-0.56		1.18	2.80	2.87	2.56	1.38	6.61	-	-	-
6	0.56-1		0.53	1.65	0.60	0.95	0.58	0.97	-	-	-
5	1-1.8		0.40	1.05	0.46	0.62	0.49	0.22	-	-	-
4	1.8-3.2		0.23	0.51	0.11	0.37	0.41	0.01	-	-	-
3	3.2-5.6		0.32	0.71	0.24	0.49	0.41	0.01	-	-	-
2	5.6-10		0.15	0.44	0.24	0.49	0.25	0.01	-	-	-
1	10-18		0.32	0.31	0.07	0.54	0.58	0.00	-	-	-
inlet	>18		0.45	0.31	1.08	1.19	2.50	0.51	-	-	-
	Total (μg)		32.01	51.43	30.34	33.90	21.35	41.63			

Py:pyrite, Mt:magnetite, Sid:siderite, TEM: for transmission electron microscopy, IA: for isotopes analysis, PTFE:polytetrafluoroethylene, Cu grid: TEM copper grid, Fe removal rate are given in mg.shot^{-1}.J^{-1}.cm^{2}

Table S2: Compilation of all experiments of aerosol collection showing the mineral analyzed, the duration of the collection (in h), the average Fe removal rate (in g.shot^{-1}.J.cm^{-2}), the purpose of the collection and the substrate used. The amount of Fe collected (in μg) is given for each impactor stage (numbered) and its corresponding size class (in μm).

Iron mass distribution (IMD) and iron isotope analysis

The PTFE filters were soaked in 1 to 2mL 8M HCl (magnetite, siderite) or *aqua regia* (8M HCl/7M HNO_3) (pyrite and pyrrhotite) to dissolve the collected particles, and rinsed with 18 MΩ water. The solution was evaporated and diluted with 0.8mL of 0.5M HCl. The IMD was determined by measuring the total iron content of each sample by colometric method using 38μL of sample in 1.5mL of *Ferrozine* solution [47]. The remaining 0.762mL of solution was evaporated, oxidized using ~25μL of 14M HNO_3, evaporated a second time and dissolved in 50μL of 0.5M HCl for standard anion-exchange chromatography using an AG1-X4 resin to purify Fe for Fe isotope analysis[26]. Iron isotope analysis was done using a Micromass Isoprobe following methods described in Beard et al. (2003). Accuracy of Fe isotope analysis was established by analysis of

73 solutions that mimicked the chemical composition of the substrate made with Fe of
74 known isotope composition. These test solutions were processed through the analytical
75 procedure and measured Fe isotope compositions matched those of the unadulterated Fe
76 [48]. Given the small amount of iron (<50μg), samples were put on small columns (400μL)
77 loaded with 7M HCl, and eluted over a single pass using 0.7mL of 0.5M HCl. Another
78 colorimetric test was conducted as an elution yield control. Test solutions containing 2μg,
79 5μg, and 10μg of Fe were made for magnetite using a High Purity Standard Fe solution
80 and for pyrite, pyrrhotite and siderite by dissolving single grains of the same batches as
81 these used for laser ablation and processing the same way as samples were. There are no
82 matrix effects associated with isotopic analysis for samples that had more than 2μg of Fe
83 based on analyses of test solutions of known Fe isotopic composition that matched the
84 chemical composition of the phases that were processed through the present study.

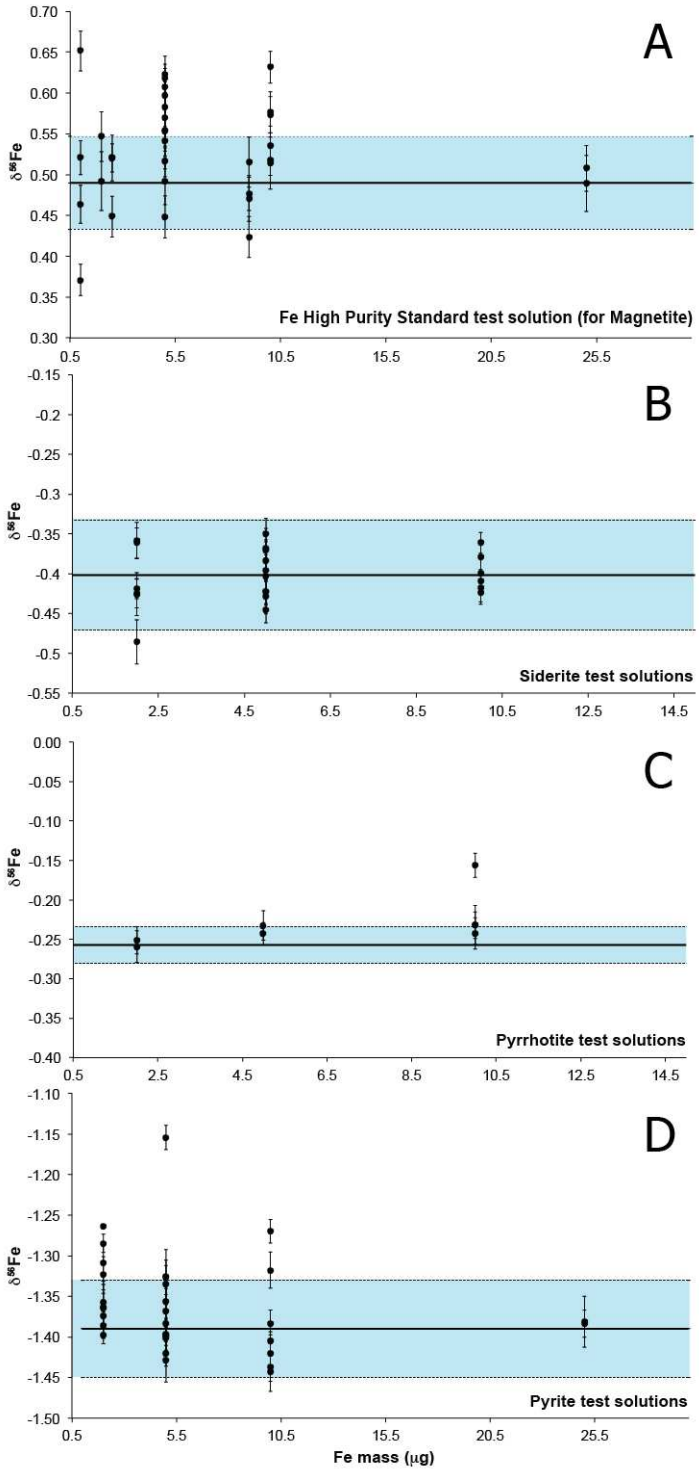

Figure S2: Measured Fe isotope composition ($\delta^{56}Fe_{igrxs}$) of test solutions made from HPS Fe standard and dissolution of pyrite, pyrrhotite and siderite. No conspicuous isotopic fractionation is observed for Fe masses over 2μg. A) HPS Fe standard tests conducted from 1mg to 25mg Fe (n=35, 2SD=0.11‰). B) Siderite tests (Geology Museum, UW Madison) conducted from 2mg to 10mg Fe (n=22, 2SD=0.07‰). C) Pyrrhotite tests (North Bend, WA) conducted from 2 to 10mg (n=8, 2SD=0.06‰). D) Pyrite tests (Balmant, NY) conducted from 2mg to 25mg (n=32, 2SD=0.12‰).

92 Samples with less Fe were combined with the nearest ones in the aerosol collection series
93 to ensure that all samples contained ≥2 μg of Fe. Removal of chlorine compounds was
94 done using 14M HNO_3 and H_2O_2, and the solutions were brought to a 25ppm Fe
95 concentration in 2% HNO_3.
96 Isotope analyses were conducted at the University of Wisconsin-Madison using solution
97 nebulization MC-ICP-MS on a Micromass *Isoprobe* equipped with a self-aspirating,
98 desolvation nebulizer (Cetac *Aridus II*) operating at ~50μLmin^{-1}. Isotopic analysis was
99 done on solutions of 600ppb Fe concentration using a standard-sample-standard
100 bracketing approach, referenced to a 600ppb High Purity Standard Fe solution, using a
101 6min washout and 0.1% HNO_3. Data are reported as δ^{56}Fe values relative to the average
102 of igneous rocks [26] as follows:

103 $$\delta^{56}Fe = \left({}^{56}Fe/{}^{54}Fe_{sample} \Big/ {}^{56}Fe/{}^{54}Fe_{IgRxs} - 1 \right) \cdot 10^3 \qquad (1)$$

104 On this scale, the IRMM-014 standard has a δ^{56}Fe value of -0.09‰ [27].
105
106 *Electron microscopy*
107 Scanning Electron Microscopy observations were conducted at the University of
108 Wisconsin-Madison using a Field Emission Gun (FEG-SEM) Leo 1530 (Zeiss-Leica,
109 Switzerland/Germany) operated at 3keV with a maximum resolution of ~3nm.
110 Transmission Electron Microscopy was conducted in the same department using a FEI
111 Titan 80-200 aberration corrected scanning/transmission electron microscope (Hillsboro,
112 OR, USA) operated at 200keV. The microscope is equipped with a Field Emission Gun, a
113 High Annular Dark Field Detector (HAADF), an Energy Dispersive X-Ray analyzer

(EDAX, Mahwah, NJ, USA) and a CCD camera (Gatan US1000XP, 2kx2k, Pleasanton, CA, USA).

Samples

	Magnetite	Siderite	Pyrrhotite	Pyrite
C	-	10.68	-	-
O	27.64	42.97	-	-
Mg	-	2.57	-	-
S	-	-	39.08	53.59
Ca	-	0.59	-	-
Mn	-	12.77	-	0.01
Fe	72.36	30.94	60.85	47.33
Ni	-	-	-	-
Cu	-	-	-	0.01
Zn	-	-	0.02	-
Total	100	100.53	99.96	100.95

Table S3: Chemical compositions of the analyzed samples determined by electron microprobe analysis, given as elemental percentages of the total mass. O and C were determined from the stoichiometry of the minerals.

Impactor stage	Size class (μm)	Exp sample	120625 Py		120627 Py		121026 Py		120726-1 Mt		121026-2 Sid		130408 Po	
			δ^{56}Fe	2SD	δ^{56}Fe	2SD	δ^{56}Fe	2SD	δ^{56}Fe	2SD	δ^{56}Fe	2SD	δ^{56}Fe	2SD
After filter	<0.056		-1.28	0.08	-1.32	0.09	-1.44	0.03	-0.56	0.04	-0.79	0.03	-0.80	0.02
10	0.056-0.1		-1.21	0.08	-1.39	0.08	-1.41	0.03	0.15	0.25				
9	0.1-0.18		-1.36	0.09	-1.31	0.09	-1.41	0.02	0.51	0.08	-0.30	0.03	-0.49	0.08
8	0.18-0.32		-1.36	0.08	-1.39	0.08	-1.34	0.05	1.29	0.04	-0.16	0.08	0.08	0.08
7	0.32-0.56				-1.33	0.08	-1.32	0.05	1.12	0.25			0.14	0.02
6	0.56-1													
5	1-1.8													
4	1.8-3.2		-0.99	0.08	-	-					-0.15	0.03		
3	3.2-5.6						-0.81	0.05	0.33	0.25			-0.07	0.01
2	5.6-10													
1	10-18													
inlet	>18										0.05	0.08		
Mass Balance			**-1.29**	0.09	**-1.33**	0.09	**-1.32**	0.04	**0.40**	0.21	**-0.33**	0.21	**-0.26**	0.14
Initial sample			*-1.39*	*0.06*	*-1.39*	*0.06*	*-1.39*	*0.06*	*0.32*	*0.05*	*-0.40*	*0.07*	*-0.26*	*0.02*

Table S4: Numerical data of δ^{56}Fe analyses of the collected aerosols for the four studied minerals. Some samples had to be combined to reach the minimum amount of iron required for processing. Uncertainties are given as 2SD of multiple analyses of the corresponding test solution. Mass balances are calculated following the equation in the text, and their uncertainty is the error propagation over all δ^{56}Fe values included in the calculation

Results

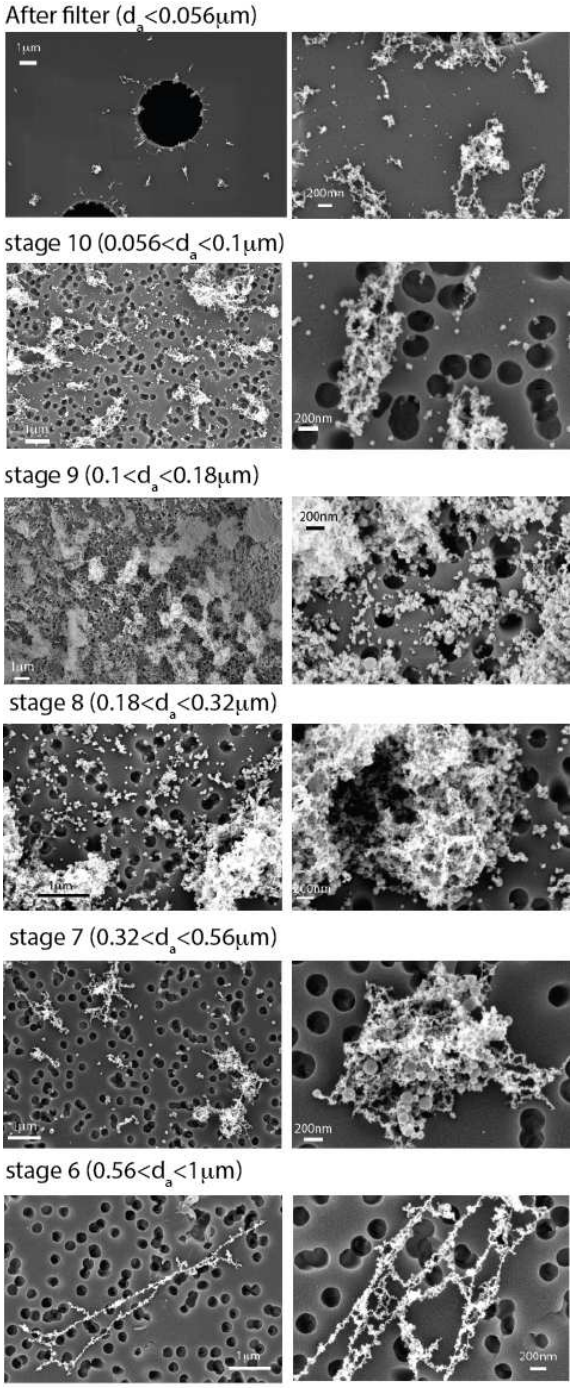

Figure S3: FEG-SEM images of laser produced aerosols from magnetite, collected on polycarbonate filters. The different stages show variable amounts of agglomerate accumulation, in agreement with the measured IMD. Agglomerates are more concentrated on stages 8 and 9, whereas finer particles are more common on stages 10 and the filter. Stage 6 only shows rare large agglomerates. Spheres also appear more numerous on stages 8 and 9, and much bigger than stages 10 and the filter. The lower δ^{56}Fe values measured for fine particle stages may be explained by a higher contribution of small, low-^{56}Fe/^{54}Fe spheres, whereas larger spheres have higher δ^{56}Fe values and high ^{56}Fe/^{54}Fe agglomerates.

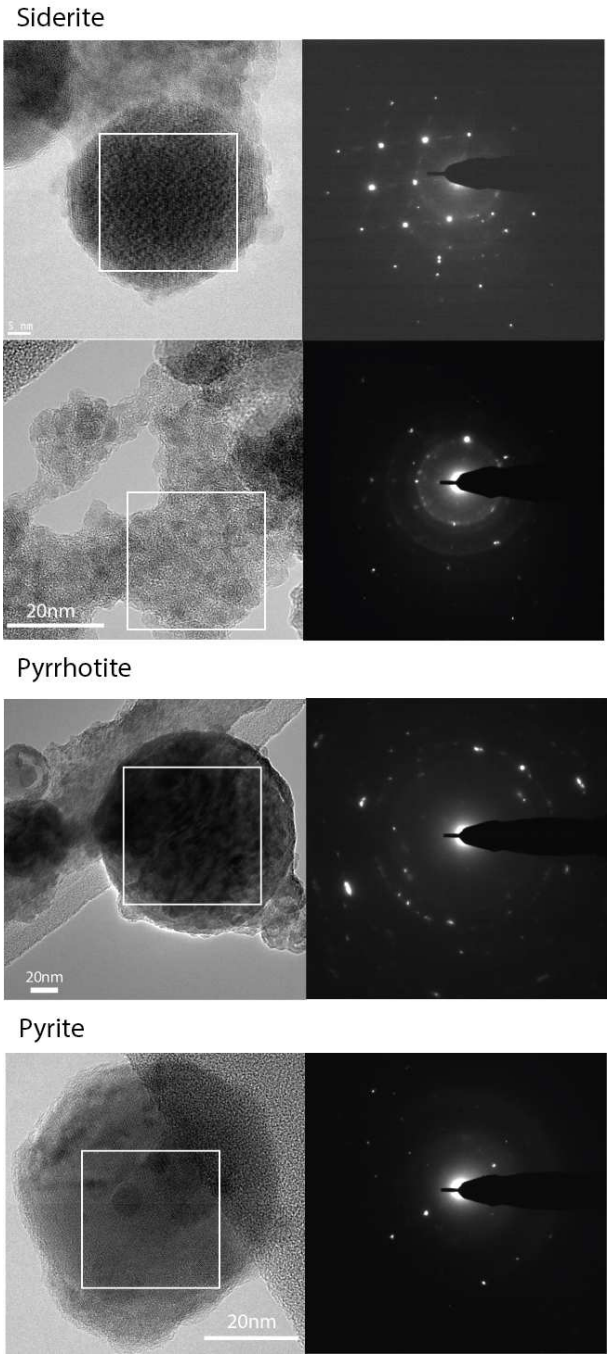

Figure S4: High resolution TEM images of particles from siderite, pyrrhotite and pyrite and their respective diffraction pattern (Fast Fourier Transform). Siderite induced spheres show a regular crystalline lattice while the agglomerates also exhibit crystallized domains, small (~5nm) and round shaped. Diffractions rings suggest a polycrystalline structure over a whole aggregate. Pyrrhotite sphere is apparently crystallized (bright spots on SAD pattern). The dim spots aligned on circles might come from the agglomerate phases coating the main sphere and could suggest a polycrystalline structure like this observed with siderite. Nevertheless, this could also be part of a multi-domain crystallized sphere. Pyrite induces crystallized spheres, yet it is difficult to find a good zone axis to perform SAD analysis due to their thickness and random orientation. The best one gives information about a possibly cubic crystalline lattice.

Annex 1:

Evaluation of ε in the case of a femtosecond laser induced plasma.

The epsilon parameter (ε) represents a condensation timescale normalized to a system cooling rate, applicable to any type of system for which the equation parameters can be defined. Following Richter (2004), the critical value for ε to have an effect on the occurrence of isotopic fraction is 10^{-3}.

$$\varepsilon = \frac{\tau_{cond}}{\tau_T}$$

τ_{cond} is the condensation timescale of the considered amount of Fe and τ_T is a timescale of the temperature change of the system.

In the same study, eq 19 states:

$$\varepsilon = \frac{\tau_{cond}}{\tau_T} = \frac{\lambda_T V_C \rho_i \eta^{-\frac{1}{3}}}{A J_{i,0}}$$

λ_T is the cooling rate of the system, Vc is the volume of the condensed phase, A is the surface area ($\underline{V_c/A}=r/3$ for a sphere of radius r), ρ_i is the molecular density of i, η is the number of particles condensing and $J_{i,0}$ is the free evaporation rate at some specified P,T conditions.

- In Le Drogoff *et al.*, λ_t depends on the laser pulse width and is of the order of ~10^9K.s^{-1} with extrema at 5.10^8 and 7.10^8 K.s^{-1}for pulse widths varying between 100fs and 270ps respectively. From this study, no other parameter influences the cooling rate in a significant manner.

- Considering the measured IMD and our observations, we can consider the particle average radius to be around 100nm. This measurement gives access to the geometric parameter of the equation: $Vc/A=3.5.10^{-8}$.

- Considering the average ablated mass per laser shot (~2.10^{-11}g.shot^{-1}) and the average mass of a spherical particle (r=100nm) of iron (ρ_{Fe}=7.1g.cm^{-3}), the number of particles generated by a single shot is of the order of η~10^9. This estimation can only be of the order of magnitude since more material is often condensing and Fe is not equally distributed into the different populations of particles (e.g. Fe/S enrichment factors varying between pyrrhotite and pyrite).

- Considering the same iron density in g.cm^{-3}, the molecular density is ρ_{Fe}=0.14.10^{-6}mol.m^{-3}

- Finally, Cohen *et al.* (2003)[49] define, for different iron species (pure Fe and Fe-oxides) a dependence of J on the temperature following an Arrhenius relation. If we consider the range of temperatures femtosecond laser induced plasma evolves through (~8000K down to, at lowest, ~2000K), we can extrapolate or read values for $J_{i,0}$ ranging from ~$10^{-1.5}$ to ~10^{-6} moles.cm^{-2}.s^{-1} respectively (abscises scale in Figure S4).

Applying the extrema values of all parameters to the calculations, ε spans between orders of magnitude of ~10^{-5} to 10^{-1} (ordinates scale in Figure S5).

This range includes the critical values of 10^{-3} for ε that is the transition from a regime where isotopic fraction is possible and one for which it is not
Interestingly, all other parameters being fixed, ε=10^{-3} gives a minimum and maximum values for $J_{i,0}$ that equal $10^{-3.6}$ and $10^{-3.3}$ respectively. When compared to Cohen *et al.* (2003), this evaporation rate corresponds to temperatures ranging from ~3300K to ~3600K. These temperatures are consistent with the boiling point of Fe for pressures above ambient conditions (3023K at atmospheric pressure).
Hence, we estimate being within the correct range of values to discuss the elemental and isotopic fractionation occurring (or not) with Fe during its condensation.

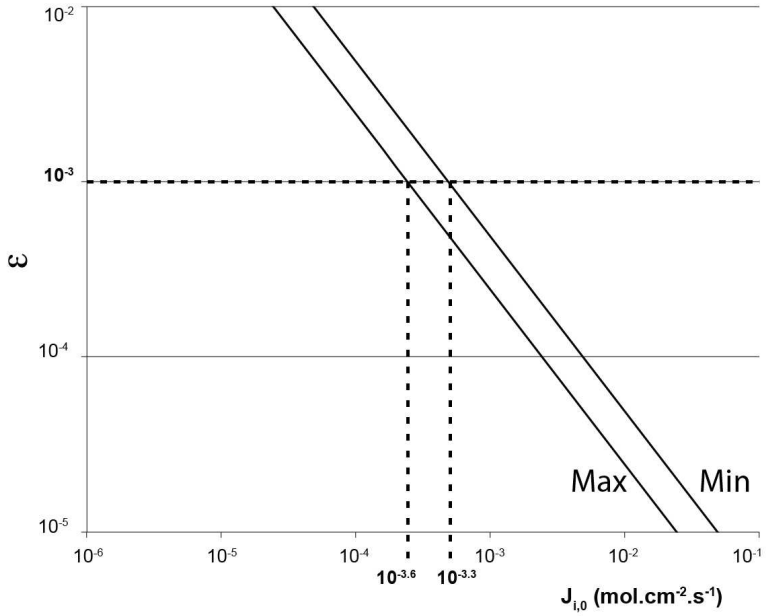

Figure S5: Epsilon (ε) factor as a function of the condensation/evaporation rate ($J_{i,0}$). The minimum curve (Min) corresponds to a calculation that takes into account the minimum cooling rate inferred from Le Drogoff et al. (2004) and the upper limit for $J_{i,0}$. The maximum curve (Max) corresponds to a calculation made using the maximum estimated cooling rate and the lower limit for $J_{i,0}$. The critical value ε=10^{-3} intersect the Min-Max area in values of $J_{i,0}$ that correspond to Fe boiling temperature at pressures above 1atm. This extrapolation is made from the representation of $J_{i,0}$ as a function of temperature in Cohen et al. (2003).